

University of Groningen

Aggregation of dicationic surfactants with methyl orange in aqueous solution

Buwalda, R.T.; Engberts, Jan

Published in:
Langmuir

DOI:
[10.1021/la001277f](https://doi.org/10.1021/la001277f)

IMPORTANT NOTE: You are advised to consult the publisher's version (publisher's PDF) if you wish to cite from it. Please check the document version below.

Document Version
Publisher's PDF, also known as Version of record

Publication date:
2001

[Link to publication in University of Groningen/UMCG research database](#)

Citation for published version (APA):

Buwalda, R. T., & Engberts, J. B. F. N. (2001). Aggregation of dicationic surfactants with methyl orange in aqueous solution. *Langmuir*, 17(4), 1054 - 1059. DOI: 10.1021/la001277f

Copyright

Other than for strictly personal use, it is not permitted to download or to forward/distribute the text or part of it without the consent of the author(s) and/or copyright holder(s), unless the work is under an open content license (like Creative Commons).

Take-down policy

If you believe that this document breaches copyright please contact us providing details, and we will remove access to the work immediately and investigate your claim.

Downloaded from the University of Groningen/UMCG research database (Pure): <http://www.rug.nl/research/portal>. For technical reasons the number of authors shown on this cover page is limited to 10 maximum.

Aggregation of Dicationic Surfactants with Methyl Orange in Aqueous Solution

Rixt T. Buwalda and Jan B. F. N. Engberts*

Physical Organic Chemistry Unit, Stratingh Institute, University of Groningen, Nijenborgh 4, 9747 AG Groningen, The Netherlands

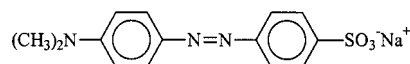
Received September 6, 2000. In Final Form: November 29, 2000

The interactions of Methyl Orange (MO) with a series of gemini bis(quaternary ammonium bromide) amphiphiles (12-*n*-12, *n* = 4, 8, 12), a pyridinium-based gemini amphiphile (10p-4-p10), a bolaform amphiphile (C₂₀Me₆), and a dicationic amphiphile lacking a second alkyl tail (12-4) in aqueous solution have been investigated by means of UV-vis spectroscopy. It was observed that aggregation of surfactant and dye takes place at surfactant concentrations far below the critical micelle concentration of the individual surfactants. Aggregation was reflected by a ca. 80 nm hypsochromic shift of the $\pi \rightarrow \pi^*$ absorption band of MO. Precipitates formed in the aqueous solutions of surfactants and dyes were isolated and consist of a surfactant to dye molar ratio of 1:2. Krafft temperatures (T_K) of surfactant-dye salts were determined by differential scanning calorimetry (DSC) and in phase penetration experiments using optical polarizing microscopy. The solution behavior of 12-*n*-12 2MO surfactants as studied by optical microscopy and DSC is dependent on the spacer length: 12-12-12 2MO dissolves at T_K whereas 12-8-12 2MO forms myelins at T_K . Moreover, 12-4-12 2MO does not dissolve at $T < 100$ °C. Similarly, 10p-4-p10 2MO does not dissolve at $T < 100$ °C. Myelins are observed for C₂₀Me₆ 2MO and for 12-4 2MO. Surfactant-dye salts 12-*n*-12 2MO (*n* = 4, 8, 12), 10p-4-p10 2MO, C₂₀Me₆ 2MO, and 12-4 2MO form vesicular structures in aqueous solutions as indicated by transmission electron microscopy. Vesicles are also formed upon mixing aqueous solutions of surfactants and MO. The types of aggregates formed in aqueous solutions of 12-*n*-12 2MO are independent of *n* since vesicles are formed in aqueous solution in all cases.

Introduction

Dye-surfactant interactions in dilute aqueous solution have been extensively studied by spectral techniques.¹ Aggregation is reflected by changes in the absorption or fluorescence spectra of the dyes. The wavelength of maximum absorption of Methyl Orange (MO, Chart 1) undergoes a blue shift upon addition of small amounts of cationic surfactants.²⁻⁷ Moreover, the shape of the new band is narrower than that of MO in pure water. Further addition of surfactant results in an absorption spectrum of the dye characteristic of that in the presence of cationic micelles. The origin of the short wavelength absorption band is still under discussion. Several explanations have evolved, but most likely, surfactant-assisted dye aggregation is responsible for the short wavelength absorption band.^{2,6} The molecular exciton theory predicts a blue shift of the $\pi \rightarrow \pi^*$ absorption band when dye molecules are arranged in a parallel fashion, the so-called H-aggregation.⁸ Apart from dye aggregation cis-trans isomerism⁴ and ion-pair formation⁵ have also been postulated to

Chart 1. Structure of Methyl Orange (MO)



account for the spectral changes. However, a conformational change of the dye upon aggregation could be ruled out on the basis of resonance Raman spectroscopy which showed that the dye retains its trans configuration upon interaction with surfactants and proteins.⁹

The short wavelength absorption band of MO can also be induced by polymers,^{10,11} proteins,¹² or polysoaps.³ Originally, MO was used as a model compound for studying the interactions of small molecules and proteins in order to obtain insight into their effect on changes in structure and properties.¹² Addition of small amounts of polymer gave rise to the largest changes in the absorption spectrum of MO. Presumably, dye aggregates are formed at low polymer concentrations which are diluted over the polymer backbone upon further addition of polymer and the absorption spectrum shifts to that of MO in apolar solvents.¹⁰

In a previous study⁶ we have investigated the interactions of cationic *n*-alkyltrimethylammonium bromide and

* To whom correspondence may be addressed. E-mail: J.B.F.N. Engberts@chem.rug.nl. Fax: +31(0)503634296.

(1) See for example: (a) Amire, O. A.; Burrows, H. D. In *Surfactants in Solution*; Mittal, K. L., Bothorel, P., Eds.; Plenum Press: New York, 1986; Vol. 4. (b) Sarkar, M.; Poddar, S. *J. Colloid. Interface Sci.* **2000**, *221*, 181.

(2) Reeves, R. L.; Harkaway, S. A. In *Micellization, Solubilization, and Microemulsions*; Mittal, K. L., Ed.; Plenum Press: New York, 1977; Vol. 4.

(3) Wang, G.-J.; Engberts, J. B. F. N. *Langmuir* **1994**, *10*, 2583.

(4) Quadrioglio, F.; Crescenzi, V. *J. Colloid Interface Sci.* **1971**, *35*, 447.

(5) (a) Dutta, R. K.; Bhat, S. N. *Bull. Chem. Soc. Jpn.* **1993**, *66*, 2457.

(b) Dutta, R. K.; Bhat, S. N. *Colloids Surf., A* **1996**, *106*, 127.

(6) Buwalda, R. T.; Jonker, J. M.; Engberts, J. B. F. N. *Langmuir* **1999**, *15*, 1083.

(7) Karukstis, K. K.; Savin, D. A.; Loftus, C. Y.; D'Angelo, N. D. *J. Colloid Interface Sci.* **1998**, *203*, 157.

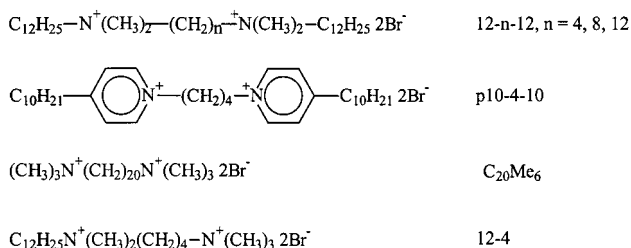
(8) McRae, E. G.; Kasha, M. *J. Phys. Chem.* **1958**, *28*, 721.

(9) Dawber, J. G.; Fischer, D. T.; Warhurst, P. R. *J. Chem. Soc., Faraday Trans. 1* **1986**, *82*, 119.

(10) (a) Yamamoto, H.; Nakazawa, A.; Hayakawa, T. *J. Polym. Sci., Polym. Lett. Ed.* **1983**, *21*, 131. (b) Takagishi, T.; Ueno, T.; Kuroki, N.; Shima, S.; Sakai, H. *J. Polym. Sci., Polym. Chem. Ed.* **1984**, *22*, 1281. (c) Yamamoto, H.; Nakazawa, A. *Biopolymers* **1984**, *23*, 1367.

(11) Klotz, I. M.; Royer, G. P.; Sloniewsky, A. R. *Biochemistry* **1969**, *8*, 4752.

(12) (a) Klotz, I. M.; Marian Walker, F.; Pivan, R. B. *J. Am. Chem. Soc.* **1946**, *68*, 1486. (b) Klotz, I. M.; Marian Walker, F. *J. Phys. Chem.* **1947**, *55*, 666. (c) Klotz, I. M. *J. Am. Chem. Soc.* **1946**, *68*, 2299. (d) Klotz, I. M.; Burkhard, R. K.; Urquhart, J. M. *J. Am. Chem. Soc.* **1952**, *74*, 202. (e) Forbes, W. F.; Milligan, B. *Aust. J. Chem.* **1962**, *15*, 841. (f) Miller, J. A.; Sapp, R. W.; Miller, E. C. *J. Am. Chem. Soc.* **1948**, *70*, 3458.

Chart 2. Used Surfactants and Their Abbreviations

4-*n*-alkyl-1-methylpyridinium iodide amphiphiles with MO and related azo dyes at low concentrations in aqueous solution. The effect of surfactant alkyl tail length on the aggregation process with azo dyes was examined in some detail. Moreover, the effect of a variation of the surfactant headgroup structure on the interactions with MO was studied. Upon changes of the structure of the azo dyes, it was observed that the position of the anionic substituent in the dye is important in the aggregation process with surfactants whereas its nature is of less influence. Moreover, the dialkylamino substituent is necessary for aggregation to occur. Although the effect of surfactant headgroup structure and alkyl chain length on the surfactant-dye aggregation process have been investigated, further structural variations in the amphiphile part have not been explored.

The present study was undertaken to examine the effect of more drastic structural variations in the amphiphile on the interactions with MO in aqueous solution. We have studied different types of amphiphiles: bis(quaternary ammonium bromide) gemini surfactants (12-*n*-12, *n* = 4, 8, 12), a pyridinium-based gemini surfactant (10p-4-p10), a bolaform surfactant (C₂₀Me₆), and a gemini analogue that lacks the second alkyl chain (12-4), (Chart 2). The morphology of the aggregates formed solely from 12-*n*-12 gemini surfactants largely depends on the spacer length (*n*).¹³ In the case of 12-*n*-12 geminis, short spacers (*n* = 2, 3) induce the formation of wormlike micelles, geminis with intermediate spacers (*s* = 4–12) form spheroidal micelles, and vesicles are formed when *n* = 16, 20. The large influence of *n* on the aggregation behavior of gemini surfactants makes them interesting for studying their aggregation with MO. Bolaform surfactants are structurally related to geminis, but the headgroups of bolaform surfactants are connected by a long alkyl chain. The alkyl spacer of bolaform surfactants is partly stretched and partly bent in micelles.¹⁴ Dicationic surfactant 12-4 is interesting since it is intermediate between a gemini surfactant and the conventional surfactant *n*-dodecyltrimethylammonium bromide.

Dye-surfactant salts were studied by differential scanning calorimetry (DSC) for determining Krafft temperatures (*T_K*), and the formation of myelins was studied in so-called phase penetration experiments using optical microscopy.¹⁵ The morphology of aggregates formed from dicationic surfactants and MO in aqueous solution was studied by transmission electron microscopy (TEM).

Experimental Section

General Remarks. ¹H NMR and ¹³C NMR spectra were measured at 200 or 300 MHz on a Varian Gemini-200 or a Varian VXR-300 MHz spectrophotometer, respectively. Column chromatography was performed using neutral Al₂O₃ (activity III)

- (13) (a) Danino, D.; Talmon, Y.; Zana, R. *Langmuir* **1995**, *11*, 1448.
 (b) Zana, R.; Talmon, Y. *Nature* **1993**, *362*, 228.
 (14) Menger, F. M.; Wrenn, S. *J. Phys. Chem.* **1974**, *78*, 1387.
 (15) Fonteijn, T. A. A.; Hoekstra, D.; Engberts, J. B. F. N. *Langmuir* **1992**, *8*, 2437.

which was prepared by addition of 4.9 mL of water to 100 g of neutral Al₂O₃. Melting points (uncorrected) were determined on a Kofler hot stage or a Mettler FP2 melting point apparatus equipped with a Mettler FP21 microscope.

UV-vis Spectroscopy. UV-vis absorption spectra were recorded on a Perkin-Elmer λ5 or λ12 spectrophotometer, equipped with a thermostated cell compartment. The MO concentration was 25 μM. Solutions were prepared in 0.02 M sodium borate buffers (pH 9.4). Experiments were performed at 30 °C, except for measurements with 10p-4-p10 which were performed at 59 °C. *T_K* of 10p-4-p10 is 51.7 °C.

Optical Microscopy. Phase penetration experiments were performed on an Olympus BX 60 polarization microscope equipped with a Linkam THMS 600 hot stage.

Transmission Electron Microscopy (TEM). Transmission electron micrographs were obtained using a JEM 1200 EX electron microscope operating at 80 kV. Samples were prepared on carbon-coated collodion grids and stained with uranyl acetate (UAc) or phosphotungstic acid (PTA).

Differential Scanning Calorimetry (DSC). DSC measurements were performed on a Perkin-Elmer DSC-7 apparatus using stainless steel pans. The reference cell contained an empty pan. Heating and cooling scans were run with scan rates of 3 deg min⁻¹.

Surface Tension Experiments. Critical micellar concentrations (cmc's) of 10p-4-p10 and 12-4 were determined by drop tensiometry using a Lauda TVT1 drop tensiometer at 58 °C (10p-4-p10) or 25 °C (12-4).

Materials. Alkanediyl- α,ω -bis(dimethyldodecylammonium bromide) Surfactants (12-*n*-12, *n* = 4, 8, 12).¹⁶ These surfactants were synthesized by refluxing *N*-dodecyl-*N,N*-dimethylamine and the appropriate α,ω -dibromoalkane in a 4:1 ratio in ethanol for 2 days (*n* = 4) or 5 days (*n* = 8, 12). The concentration in α,ω -dibromoalkane was ca. 0.3 M. The reaction was followed by ¹H NMR spectroscopy and was stopped when complete conversion of α,ω -dibromoalkane had occurred. After evaporation of the solvent, the product was purified by column chromatography. Excess *N*-dodecyl-*N,N*-dimethylamine was eluted with CH₂Cl₂. Subsequent elution with CH₂Cl₂/10% MeOH gave both monoalkylated product and the desired gemini amphiphile. Surfactant fractions which contained monoalkylated product were recrystallized from CH₃CN. Gemini surfactants 12-*n*-12 were obtained as white solids in 70–75% yield. The surfactants were pure as determined by ¹H NMR spectroscopy: 12-4-12, mp 225–228 °C (dec), lit. 215 °C (dec),¹⁷ 237–240 °C;¹⁸ 12-8-12, mp 192–195 °C, lit. 206–208 °C;¹⁸ 12-12-12, mp 129–134 °C, lit. 137–138 °C.¹⁸ Melting points differ from literature values although those values show mutual differences themselves. Most likely, the differences can be attributed to the presence of traces of water in the gemini surfactants. The purity of gemini 12-12-12 was checked by elemental analysis. Anal. Calcd for C₄₀H₈₆N₂Br₂ (754.94): C, 63.64; H, 11.48; N, 3.71; Br, 21.17. Found: C, 63.50; H, 11.55; N, 3.85; Br, 21.11.

Eicosane-1,20-bis(trimethylammonium) Dibromide (C₂₀Me₆).¹⁹ Bola amphiphile C₂₀Me₆ was synthesized according to a literature procedure.¹⁴ In short, 300 mg (0.68 mmol) of 1,20-dibromoeicosane²⁰ was added to 6 mL of a 33% ethanolic solution of dimethylamine. The solution was refluxed for 48 h after which the reaction was complete as indicated by ¹H NMR spectroscopy. The reaction mixture was cooled to room temperature and after addition of 15 mL of diethyl ether, precipitation of C₂₀Me₆ occurred. The product was isolated by suction as white crystals in 93% yield (350 mg, 0.63 mmol). Bola amphiphile C₂₀Me₆ was pure as determined by ¹H NMR spectroscopy. Mp >230 °C.

***N,N*-(1,4-Butanediyl)bis(4-decylpyridinium) Dibromide (10p-4-p10).** A solution of 1.99 g (9.1 mmol) of 4-*n*-decylpyridine²¹

- (16) Zana, R.; Benraou, M.; Rueff, R. *Langmuir* **1991**, *7*, 1072.
 (17) Menger, F. M.; Keiper, J. S.; Azov, V. *Langmuir* **2000**, *16*, 2062.
 (18) Wettig, S. Personal communication.
 (19) Yasuda, M.; Ikeda, K.; Esumi, K.; Meguro, K. *Bull. Chem. Soc. Jpn.* **1989**, *62*, 3648.
 (20) Pattison, F. L. M.; Stothers, J. B.; Woolford, R. G. *J. Am Chem. Soc.* **1956**, *2255*.
 (21) 4-*n*-Decylpyridine was synthesized according to: Sudhölter, E. J. R.; Engberts, J. B. F. N. *J. Phys. Chem.* **1979**, *83*, 1854.

and 0.66 g (3.1 mmol) of 1,4-dibromobutane in 7 mL of absolute ethanol was refluxed for 24 h under a nitrogen atmosphere. After evaporation of the solvent, the reaction mixture was purified by column chromatography. Excess 4-*n*-decylpyridine was removed by CH_2Cl_2 ; the product was eluted with $\text{CH}_2\text{Cl}_2/10\%$ MeOH. The product was recrystallized from CH_3CN in order to remove monoalkylated compound. As indicated by elemental analysis, part of the bromide counterions (<5%) had been exchanged for chloride. Therefore, 10p-4-p10 was subjected to ion exchange using a Dowex 1×8 200–400 mesh column in the Br^- form. After evaporation of the solvent, white crystalline 10p-4-p10 was obtained in a 66% yield (1.34 g, 2.04 mmol). Mp 206–208 °C (dec). ^1H NMR (200 MHz, CDCl_3): δ 0.85 (t, 6H, CH_3), 1.24–1.28 (m, 28H CH_2 alkyl tails), 1.65 (m, 4H, β - CH_2 alkyl tail), 2.42 (m, 4H, $\text{N}^+\text{CH}_2\text{CH}_2$), 2.82 (t, 4H, α - CH_2 alkyl tail), 5.09 (m, 4H, N^+ - CH_2), 7.74 (d, 4H, CH ar), 9.67 (d, 4H, CH ar). ^{13}C NMR (200 MHz, CDCl_3): δ 12.59 (p), 21.13, 26.44, 27.57, 27.68, 27.72, 27.85, 27.97, 28.03, 30.31, 34.41, 57.86 (s), 126.34 (t), 143.20 (t), 161.61 (q). Anal. Calcd for $\text{C}_{34}\text{H}_{58}\text{N}_2\text{Br}_2$ (654.66): C, 62.38; H, 8.93; N, 4.28; Br, 24.41. Found: C, 62.30; H, 8.82; N, 4.43; Br, 24.24.

***N*-Dodecyl-*N,N,N,N,N*-pentamethyl-*N,N*-butanedilammonium Dibromide (12-4).** A solution of 2.1 g (10.8 mmol) of *N*-(4-bromobutyl)-*N,N,N*-trimethylammonium bromide²² and 2.74 g (12.9 mmol) of *N*-dodecyl-*N,N*-dimethylamine in 40 mL of absolute ethanol was heated under reflux. After 72 h the ratio of starting compounds to product was constant as indicated by ^1H NMR spectroscopy and the reaction was stopped. Separation of the products was achieved by column chromatography. Excess *N*-dodecyl-*N,N*-dimethylamine was eluted with CH_2Cl_2 . Subsequently, $\text{CH}_2\text{Cl}_2/15\%$ MeOH was used for elution of the product. After removal of the solvents, 12-4 was obtained as a hygroscopic white solid (mp 215–217 °C) in 62% yield (3.27 g, 6.7 mmol). ^1H NMR (200 MHz, CD_3OD): δ 0.87 (t, 3H, CH_3), 1.25–1.35 (m, 18H, CH_2 alkyl tail), 1.75 (m, 2H, β - CH_2), 2.08 (m, 4H, CH_2), 3.31 (s, 6H, $\text{N}^+(\text{CH}_3)_2$), 3.43 (m, 11H, $\text{N}^+(\text{CH}_3)_3$ and α - CH_2). ^{13}C NMR (200 MHz, CD_3OD): δ 11.54 (p), 17.76, 18.17, 20.75, 20.82, 24.54, 27.38, 27.55, 27.70, 27.74, 27.83, 30.15 (s), 48.41, 50.78, 50.85, 50.93 (p), 61.41, 62.92, 63.80 (s). Anal. Calcd for $\text{C}_{21}\text{H}_{48}\text{N}_2\text{Br}_2$ (488.43): C, 51.64; H, 9.91; N, 5.74; Br, 32.72. Found: C, 51.13; H, 9.77; N, 5.73; Br, 32.67.

Surfactant–Dye Salts. Surfactant–MO salts were obtained by isolating precipitates formed in aqueous solutions of surfactant and MO. Typically, 40 mL of a 1.2 mM aqueous solution of MO was added to 40 mL of an aqueous solution of 0.6 mM of surfactant at 60 °C. The solution was cooled to room temperature. Crystals were isolated by suction. The purity of the surfactant–MO salt was checked by ^1H NMR spectroscopy. As indicated by this technique, the ratio of surfactant to dye was 1:2 in each case, which was to be expected on the basis of the charges of both components.

12-*n*-12 2MO. 12-4-12 2MO. Mp 245–257 °C. ^1H NMR (300 MHz, DMSO, 50 °C): δ 0.89 (t, 6H, CH_3), 1.31 (m, 36H, CH_2 alkyl chain), 1.72 (m, 4H, CH_2), 2.71 (s, 12H, $\text{N}(\text{CH}_3)_2$), 3.04 (s, 18H, $\text{N}^+(\text{CH}_3)_3$), 3.28 (m, 4H, CH_2), 6.86 (d, 4H, CH ar), 7.68–7.84 (m, 12H, CH ar). Mp's of 12-8-12 2MO and 12-12-12 2MO are 188–193 and 208–210 °C, respectively.

^1H NMR data for 12-8-12 2MO and 12-12-12 2MO are similar but differ in integration of the signal at 1.31 ppm, which is larger due to the presence of additional CH_2 groups in the spacer.

10p-4-p10 2MO. Mp 189–194 °C. ^1H NMR (300 MHz, CD_3OD): δ 0.77 (t, 6H, CH_3), 1.18 (m, 14H, CH_2 alkyl tails), 1.57 (m, 4H, CH_2), 1.96 (m, 4H, CH_2 spacer), 2.76 (t, 4H, CH_2), 2.99 (s, 12H, $\text{N}(\text{CH}_3)_2$), 4.48 (m, 4H, $\text{N}^+(\text{CH}_2)$), 6.76 (d, 4H, CH ar), 7.68–7.81 (m, 14H, CH ar). 8.66 (d, 4H, CH ar).

C_{20}Me_6 2MO. Mp 249–251 °C. ^1H NMR (300 MHz, DMSO, 50 °C): δ 1.31 (m, 32H, $(\text{CH}_2)_{16}$), 1.73 (m, 4H, CH_2), 3.08 (s, 12H, $\text{N}(\text{CH}_3)_2$), 3.24 (m, 22H, $\text{N}^+(\text{CH}_3)_3$ and N^+CH_2), 6.86 (d, 4H, ar), 7.74 (d, 8H, CH ar), 7.81 (d, 4H, CH ar).

12-4 2MO. Mp 259–265 °C. ^1H NMR (300 MHz, CD_3OD): δ 0.87 (3H, t, CH_3), 1.27 (m, 18H, CH_2 alkyl chain), 1.72 (m, 2H, CH_2), 1.83 (m, 4H, CH_2), 3.22–3.46 (m, 4H, CH_2N^+), 3.06 (s, 6H, $\text{N}(\text{CH}_3)_2$), 6.83 (d, 2H, CH ar), 7.84 (m, 4H, CH ar), 7.93 (d, 2H, CH ar).

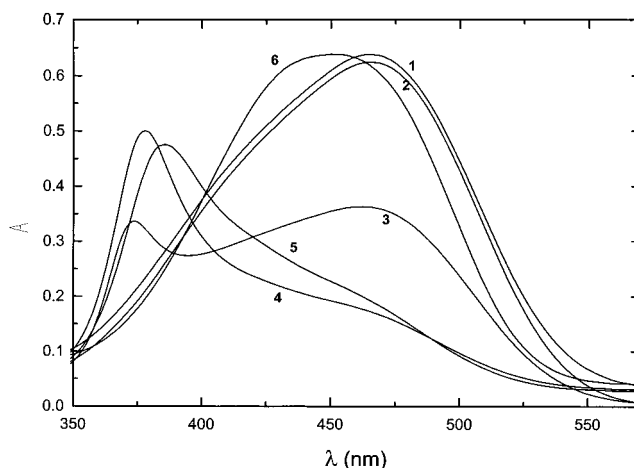


Figure 1. Effect of C_{20}Me_6 on the absorption spectrum of MO in aqueous solution at 30 °C, $[\text{MO}] = 25 \mu\text{M}$. $[\text{C}_{20}\text{Me}_6]$ (M): (1) 0, (2) 1.0×10^{-5} , (3) 6.0×10^{-5} , (4) 1.1×10^{-3} , (5) 6.0×10^{-3} , (6) 29×10^{-3} .

Results and Discussion

UV–vis Experiments. MO can be used as a solvatochromic micropolarity reporter molecule since its absorption spectrum is sensitive to medium effects. The long wavelength absorption band (λ_{max}) of MO shifts to shorter wavelengths upon decreasing the polarity of the medium in which the probe sits. Thus, in water λ_{max} is situated at 463 nm whereas it is positioned at 417 nm in ethanol. This property makes MO also useful for reporting the presence of surfactant aggregates in aqueous solution. When bound to micelles composed of cationic surfactants, λ_{max} is positioned at ca. 430 nm, which is 33 nm blue shifted to that of MO in water.

The effects of different surfactants (Chart 2) on the absorption spectrum of MO have been investigated by UV–vis spectroscopy. Figure 1 shows the effect of different concentrations of eicosane-1,20-bis(trimethylammonium) dibromide (C_{20}Me_6) on the absorption spectrum of MO. Analogous to *n*-alkyltrimethylammonium bromide and 4-*n*-alkyl-1-methylpyridinium iodide surfactants,⁶ successive additions of C_{20}Me_6 decrease the intensity of the absorption band at 463 nm. Further addition of surfactant leads to the appearance of a new band at ca. 380 nm. This short wavelength absorption band first increases and then decreases in intensity upon still further increasing the surfactant concentration, and finally it is replaced by the micellar band at ca. 430 nm. Our results indicate that for bolaform surfactants aggregation similar to that of *n*-alkyltrimethylammonium bromide surfactants is observed.^{2,3,6,7} Interestingly, the short wavelength absorption band is not observed when small amounts of *n*-decyltrimethylammonium bromide (C_{10}TAB), which is half of the C_{20}Me_6 molecule, are added. In that case, λ_{max} of MO gradually shifts from that in water to that of MO in the presence of cationic micelles. This may be explained by considering the large difference in cmc values: the cmc of C_{20}Me_6 ¹⁹ is 7.5 mol kg^{-1} whereas C_{10}TAB has a cmc of 60.2 mM.²³ The alkyl groups of bolaform surfactants are partly stretched in aggregates and therefore they are less exposed to water than the alkyl moieties of conventional surfactants in aggregates. This might explain both the lowering in cmc for bolaform surfactants compared to conventional ones and the fact that C_{20}Me_6 shows interactions with MO below the cmc whereas the interactions are absent in the case of C_{10}TAB .

(22) Thanei-Wyss, P.; Waser, P. G. *Helv. Chim. Acta* **1983**, *66*, 2189.

(23) Berr, S. S.; Caponetti, E.; Johnsson, J. S., Jr.; Jones, R. R. M.; Magid, L. D. *J. Phys. Chem.* **1986**, *90*, 5766.

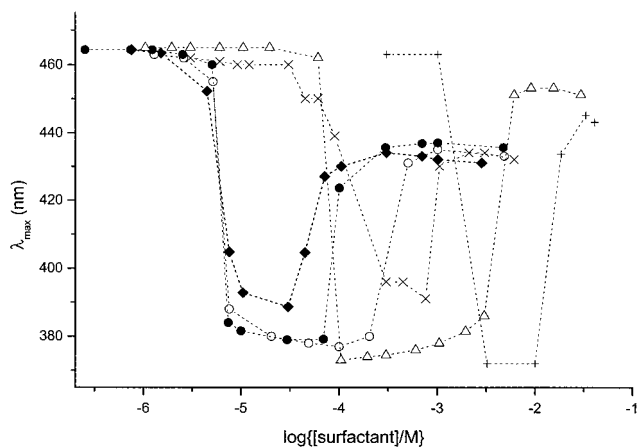


Figure 2. Effect of dicationic amphiphiles on the position of the wavelength of maximum absorption of MO in aqueous solution: (◆) 12-12-12; (●) 12-8-12; (○) 12-4-12; (×) p10-4-10; (Δ) C₂₀Me₆; (+) 12-4.

Figure 2 shows the effects of 12-*n*-12, 10p-4-p10, C₂₀Me₆, and 12-4 on the wavelength of maximum absorption of MO. The surfactants all induce the short wavelength absorption band in the absorption spectrum of MO. For 12-*n*-12 geminis the surfactant concentration necessary for aggregation to occur decreases slightly with the spacer length: cmc's of 12-*n*-12 and MO (at a MO concentration of 25 μM) are 7, 5, and 4 μM for 12-4-12, 12-8-12, and 12-12-12, respectively. The cmc decreases¹⁶ in the series 12-4-12 to 12-12-12 due to penetration of the spacer between the alkyl chains. Therefore, the decrease in aggregation concentration of 12-*n*-12 geminis and MO upon increasing *n* reflects an increase in hydrophobicity of the surfactant in this series. This is in accordance with previous studies which showed that hydrophobic interactions are important in the aggregation process of surfactants and dyes.⁶ Similar behavior is observed for 10p-4-p10. This shows that a change in the type of headgroup has no influence on the aggregation process, in accordance with previous work that showed that a change in headgroup from trimethylammonium to pyridinium has no large influence on the aggregation process.⁶ Dicationic surfactant 12-4 also shows interactions with MO below its cmc (24.1 mM).

Most likely, the short wavelength absorption band is caused by dye aggregation although there is no direct information on the structure of surfactant-dye aggregates formed at low surfactant concentration. Dye aggregation has been proposed to be responsible for the short wavelength absorption band of MO in the presence of surfactants,^{2,6} polymers,^{10,11} and proteins.¹² A hypsochromic shift in the absorption spectrum of dendrimers derivatized with azobenzene moieties has also been ascribed to interactions between the chromophores.²⁴ Similarly, the hypsochromic shift of λ_{max} upon aggregation of azobenzene-based surfactants has been attributed to aggregation of the chromophoric units.²⁵ Moreover, parallel orientation of azobenzene units in cast films of an azobenzene-containing

Table 1. Krafft Temperatures As Determined by Optical Microscopy (T_{myelin}) and DSC (T_K) and Melting Points (mp) of Surfactant 2MO Salts

compound	T_{myelin} (°C)	T_K (°C)	mp (°C)
12-4-12 2MO	<i>a</i>	<i>b</i>	254–257
12-8-12 2MO	86	87.6	188–193
12-12-12 2MO	86 ^c	85.6	208–210
P10-4-10 2MO	<i>a</i>	<i>b</i>	189–194
C ₂₀ Me ₆ 2MO	78	80.5	249–251
12-4 2MO	<23	22.1 ^d	259–265

^a No myelin formation at $T < 100$ °C. ^b No transition in the DSC enthalpogram from 0 to 100 °C. ^c Compound dissolves without the formation of myelins. ^d Weak transition.

amphiphile has been verified by X-ray diffraction experiments.²⁶ MO molecules in Langmuir–Blodgett films composed of cationic surfactants and MO are oriented in a more or less parallel fashion and show a blue shift of the $\pi \rightarrow \pi^*$ absorption band as well.²⁷

Surfactant–Dye Salts. Precipitates formed in aqueous solutions of cationic surfactants and dyes were isolated in a surfactant to dye molar ratio of 1:2. In analogy with alkyltrimethylammonium–MO surfactants,⁶ the aggregation behavior of the new surfactants was studied by optical microscopy, DSC, and TEM. The possible formation of myelins can be studied in a so-called phase penetration experiment using optical polarization microscopy.¹⁵ Water is brought into contact with solid surfactant material and, upon heating, the formation of myelins at the boundary of the crystal/water interphase can be observed. Myelins are wormlike structures and have been proposed to consist of surfactant layers alternating with water layers which are wrapped around a core axis of water.²⁸ Myelin formation can also be detected by DSC. The temperature of myelin formation (T_{myelin}) corresponds to an endothermic transition in the DSC enthalpogram.¹⁵ The solubility of surfactant–dye salts in aqueous solution shows a sudden increase when heated above T_{myelin} . Therefore, myelin formation can be compared to the Krafft temperature phenomenon for micellar systems when T_{myelin} is defined as the temperature above which the solubility of micelle-forming surfactants shows a drastic increase. Therefore, we contend that the myelin temperature of bilayer-forming surfactants corresponds to the Krafft temperature (T_K) of micelle-forming surfactants. Table 1 presents the critical temperatures as determined by DSC (T_K) and optical microscopy (T_{myelin}) as well as the melting points (mp) of the surfactant–MO salts.

Critical temperatures as determined by DSC and optical microscopy are in good agreement. The solution behavior of 12-*n*-12 2MO surfactants is dependent on the spacer length: the Krafft temperature increases upon decreasing *n* from 12 to 8, whereas 12-4-12 2MO does not dissolve at all. Moreover, 12-8-12 2MO forms myelins at T_{myelin} whereas 12-12-12 2MO dissolves at T_{myelin} . Although the difference in T_K for 12-8-12 2MO and 12-12-12 2MO is not large, it can be reproduced in DSC measurements. Both the degree of counterion binding and the nature of the counterion have been shown to affect T_{myelin} of di-*n*-alkyl phosphates.¹⁵ T_{myelin} increases upon increasing the counterion binding: T_K values for sodium di-*n*-alkyl phosphates

(24) (a) Schenning, A. P. H. J.; Elissen, Román, C.; Weener, J. W.; Baars, M. W. P. L.; Van der Gaast, S. J.; Meijer, E. W. *J. Am. Chem. Soc.* **1998**, *120*, 8199. (b) Tsuda, K.; Dol, G. C.; Gensch, T.; Hofkens, J.; Laterni, L.; Weener, J. W.; Meijer, E. W.; De Schrijver, F. C. *J. Am. Chem. Soc.* **2000**, *122*, 3445.

(25) (a) Shimomura, S.; Kunitake, T. *J. Am. Chem. Soc.* **1987**, *109*, 5157. (b) Shimomura, S.; Ando, R.; Kunitake, T. *Ber Bunsen-Ges. Phys. Chem.* **1983**, *87*, 1134. (c) Shimomura, S.; Kunitake, T. *Chem. Lett.* **1981**, 1001. (d) Everaars, M. D.; Marcelis, A. T. M.; Sudhölter, E. J. R. *Liebigs Ann. Recl.* **1997**, *21*. (e) Song, S.; Perlstein, J.; Whitten, D. G. *J. Am. Chem. Soc.* **1997**, *119*, 9144.

(26) (a) Shimomura, M.; Aiba, S.; Tajima, N.; Inoue, N.; Okuyama, K. *Langmuir* **1995**, *11*, 969. (b) Kunitake, T.; Shimomura, M.; Kajiyama, T.; Harada, A.; Okuyama, K.; Takayanagi, M. *Thin Solid Films* **1984**, *121*, L89–L91.

(27) (a) Takahashi, M.; Kobayashi, K.; Takaoka, K.; Tajima, K. *Langmuir* **1997**, *13*, 338. (b) Takahashi, M.; Kobayashi, K.; Takaoka, K.; Tajima, K. *J. Colloid Interface Sci.* **1998**, *203*, 311.

(28) Sakurai, I.; Suzuki, T.; Sakurai, S. *Biochim. Biophys. Acta* **1989**, *985*, 101.

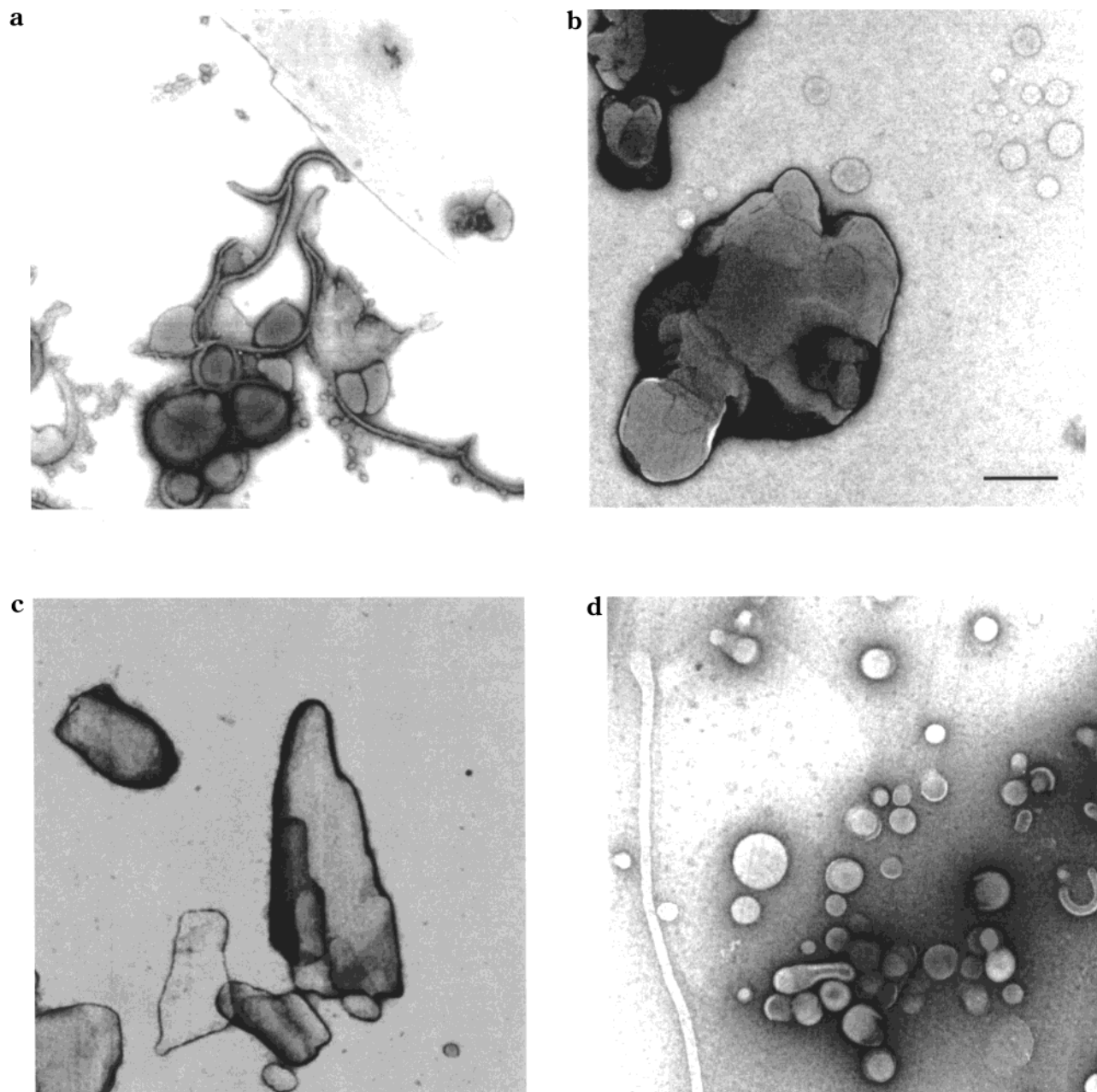


Figure 3. Negatively stained electron micrographs of aggregates formed in aqueous solutions of (a) $C_{20}Me_6$ 2MO, (b) 12-4-12 2MO, (c) 12-12-12 2MO, and (d) 0.6 mM of 12-4 and 1.2 mM of MO. Bar corresponds to 500 nm; the same magnification applies to all photographs.

are higher than those of their corresponding potassium analogues. An increase in counterion binding results in less hydrated headgroups, and this hampers the penetration of water into the crystal. Moreover, Ca^{2+} binds so strongly that calcium di-*n*-dodecyl phosphate does not form myelins upon water penetration. The degree of bromide counterion binding to 12-*n*-12 surfactants decreases in the series $n = 4, 8, 12$.¹⁶ Most likely, the MO counterion binding will also follow this trend. This explains the difference in T_K for the 12-*n*-12 2MO surfactants: 12-12-12 2MO will show the lowest degree of counterion binding and therefore it displays a lower T_K than 12-8-12. Apparently the binding affinity of MO for 12-4-12 is so high that hydration does not take place and myelin formation is inhibited. Thus, the spacer length has a profound influence on the solution behavior of 12-*n*-12 2MO surfactants in an aqueous environment as indicated by DSC and optical microscopy. Most likely, the absence of myelin formation for 10p-4-p10 2MO can also be

explained by a high binding constant of MO and 10p-4-p10. No water can penetrate the headgroup region, and lyotropic mesophases are not formed. The formation of myelins was also observed for $C_{20}Me_6$ 2MO and for 12-4 2MO although T_K was accompanied by only a weak transition in the DSC enthalpogram due to its low solubility in water.

The morphology of aggregates formed from surfactant-dye salts was investigated by TEM. Surfactant solutions were prepared by addition of 0.5 mL of water to 2–3 mg of the surfactant 2MO salts. The mixtures were heated to ca. 80 °C, and the mixtures were vortexed for several seconds to aid the dissolution of the surfactant material. Suspensions were formed in each case due to the low solubility of the surfactant-dye salts. When studied by TEM, the surfactant-dye salts were all found to form vesicular structures in aqueous solution. Vesicles show a rather large size distribution with diameters ranging from 25 nm to 1 μ m. In addition, crystals of 200 nm to 1.5 μ m

in width and several micrometers in length were often observed. Crystals were not observed for 12-4 2MO by TEM, but the solution contained crystals on visual inspection. Probably, the crystals were too large and flowed off the grid during the blotting process. Panels a–c of Figure 3 show types of aggregates that are observed in aqueous solutions of C₂₀Me₆ 2MO, 12-4-12 2MO, and 12-12-12 2MO, respectively. In a sample taken from an aqueous solution of C₂₀Me₆ 2MO different types of aggregates are observed: spherical vesicles of 30–500 nm in diameter, long wormlike vesicular structures of 30–500 nm in diameter and several micrometers in length, and sheets of several micrometers in width and length (Figure 3a). Sometimes, the tubular vesicular structures are wrapped around spherical vesicles. Surprisingly, vesicles are also formed in an aqueous solution of 12-4-12 2MO (Figure 3b) and in an aqueous solution of 10p-4-p10 2MO. In addition, crystals are observed. Both compounds failed to show myelin formation. Also the transition for myelin formation in the DSC enthalpogram was absent for both compounds. Interestingly, vesicles were observed in an aqueous solution of 12-12-12 2MO although the electron micrographs were dominated by sheets and crystals (Figure 3c). The formation of myelins for 12-12-12 2MO in phase penetration experiments was not observed. Indeed, myelin formation is apparently not an absolute prerequisite for vesicle formation.²⁹ The dependence of the solution behavior of 12-*n*-12 2MO surfactants on *n* as observed in phase penetration experiments is not found for the aggregation behavior of these surfactants in dilute aqueous solution. Vesicle formation is observed for each of the 12-*n*-12 2MO salts in aqueous solution.

The morphology of aggregates formed in aqueous mixtures of dicationic surfactants and MO was also studied by TEM. In this case, solutions were prepared by mixing aqueous solutions of surfactants and dyes in a 2:1 molar ratio. The surfactant concentration was 0.6 mM whereas the MO concentration was 1.2 mM. Aqueous solutions of surfactants and dyes are only stable for several hours after which precipitation occurs. However, aqueous solutions containing 12-4 and MO are stable for ca. 5 days. Samples taken from aqueous mixtures of 12-*n*-12 geminis and MO show the formation of spherical vesicles and crystals. Both types of aggregates show a rather large size distribution similar to that observed for surfactant–dye salts. An aqueous solution of 10p-4-p10 and MO only shows the formation of vesicles ranging in diameter from 300 nm to 1.5 μm. Aqueous mixtures of 12-4 and MO show spherical vesicles of 30 nm to 1 μm in diameter and wormlike vesicular structures of 50–100 nm in diameter and of several micrometers in length. Figure 3d shows a negatively stained electron micrograph of aggregates formed in an aqueous solution of 12-4 and MO in a mixing ratio of 1:2. Whereas an aqueous solution of C₂₀Me₆ 2MO displayed different types of vesicular structures, spherical vesicles of 100 nm to 1 μm in diameter were observed in an aqueous mixture of C₂₀Me₆ and MO (1:2, containing an equivalent of NaBr). In addition, crystals of 500 nm to 1 μm in width and of several micrometers in length were observed in aqueous mixtures of the bolaform amphiphile

and MO. Types of aggregates formed in aqueous solutions of surfactant–dye salts and their dimensions are similar to those formed in aqueous mixtures of surfactants and MO for 12-4-12 2MO and 12-8-12 2MO. Vesicles and crystals are observed in aqueous solutions of 10p-4-p10 2MO and 12-4 2MO whereas only vesicular structures are observed in aqueous mixtures of 10p-4-p10 and 12-4 and MO. However, 10p-4-p10 2MO crystallizes a few hours after mixing whereas precipitation takes several days in the case of an aqueous solution of 12-4 and MO.

Upon interaction with the hydrophobic MO counterions the preference of the studied surfactants changes from micelles¹⁶ to vesicular structures. Apparently, the shape of the surfactant molecules changes from conical to cylindrical. The effective headgroup area decreases due to electrostatic interactions between the ionic groups and the volume of the apolar part increases. This corresponds to an increase in the value of the packing parameter *P* which relates the shape of the surfactant to the morphology that the aggregate will adopt in aqueous solution.³⁰ *P* can be calculated using eq 1

$$P = V/a_0l \quad (1)$$

where *V* is the volume of the hydrocarbon part of the surfactant, *l* its alkyl chain length, and *a*₀ the mean cross-sectional headgroup surface area. Surfactants with 0 < *P* < 1/3 form micelles in aqueous solution, 1/3 < *P* < 1/2 indicates the formation of wormlike micelles, and surfactants with 1/2 < *P* < 1 display vesicle formation. Furthermore, we note that counterion-induced morphology changes for conventional surfactants from spherical to wormlike micelles have been described.³¹ Morphology changes from spherical micelles to vesicles as induced by counterions have also been studied, although less extensively.³² To the best of our knowledge, the aggregation behavior of gemini and bolaform surfactants with hydrophobic counterions has not been reported before. Moreover, this is one of the few examples of vesicle formation in aqueous solutions of gemini and bolaform surfactants which form micelles by themselves. Vesicles are formed in aqueous solutions of an anionic gemini surfactant and hexadecyltrimethylammonium bromide³³ and upon addition of hexanol to an aqueous solution of gemini surfactant 12-2-12.³⁴ On the other hand, mixed micelles of gemini and monomeric surfactants have been extensively studied.³⁵ Similar experiments on bolaform and nonbolaform amphiphiles have been performed.³⁶

LA001277F

(30) Israelachvili, J. N.; Mitchell, D. J.; Ninham, B. W. *J. Chem. Soc., Faraday Trans. 2* **1976**, *72*, 1525.

(31) (a) Gravsholt, S. *J. Colloid Interface Sci.* **1976**, *57*, 575. (b) Bijma, K.; Rank, E.; Engberts, J. B. F. *N. J. Colloid Interface Sci.* **1998**, *205*, 245.

(32) (a) Mishra, B. K.; Samant, S. D.; Pradhan, P.; Mishra, S. B.; Manohar, C. *Langmuir* **1993**, *9*, 894. (b) Lin, Z.; Cai, J. J.; Scriven, L. E.; Davis, H. T. *J. Phys. Chem.* **1994**, *98*, 5984.

(33) Zana, R.; Lévy, H.; Danino, D.; Talmon, Y.; Kwetkat, K. *Langmuir* **1997**, *13*, 402.

(34) Oda, R.; Bourdieu, L.; Schmutz, M. *J. Phys. Chem. B* **1997**, *101*, 5913.

(35) (a) De, S.; Aswal, V. K.; Goyal, P. S.; Battacharya, S. *J. Phys. Chem. B* **1997**, *101*, 5639. (b) Schosseler, F.; Anthony, D.; Beinert, G.; Zana, R. *Langmuir* **1995**, *11*, 3347. (c) Zhao, J.; Christian, S. D.; Fung, B. M. *J. Phys. Chem. B* **1998**, *102*, 7613.

(36) Visscher, I.; Engberts, J. B. F. *N. Langmuir* **2000**, *16*, 52.

(29) Roosjen, A. Personal communication.